Observation of Photon-Induced W Boson Pair Production

HEP Seminar, QMUL

Philip Sommer

University of Sheffield

12.11.2020

Introduction

- Recently, ATLAS published a set of landmark results
- Using the LHC as a photon collider

- Previous or similar studies:

$\gamma\gamma \to \ell\ell$	Phys. Lett. B 749 (2015) 242	pp @ 7 TeV
$\gamma\gamma \to WW$	Phys. Rev. D 94 (2016) 032011	pp @ 8 TeV
$\gamma\gamma \to \mu\mu$	Phys. Lett. B 777 (2018) 303	pp @ 13 TeV
$\gamma\gamma \to \mu\mu$	Phys. Rev. Lett. 121 (2018) 212301	PbPb @ 5.02 TeV
$\gamma\gamma \to \gamma\gamma$	Phys. Rev. Lett. 123 (2019) 052001	PbPb @ 5.02 TeV
$\gamma\gamma \to \gamma\gamma$	arXiv:2008.05355 (new!)	PbPb @ 5.02 TeV
$\gamma\gamma \to \ell\ell$	arXiv:2009.14537 (new!)	pp @ 13 TeV

C Physics Technology Community In focus Magazine Jobs

HIGGS AND ELECTROWEAK | NEWS

The LHC as a photon collider

15 August 2020

A report from the ATLAS experiment

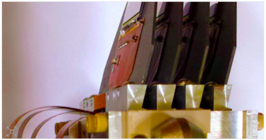

Future forward Part of the ATLAS forward-proton spectrometer. Credit: ATLAS collaboration

Protons accelerated by the LHC generate a large flux of quasi-real high-energy photons that can interact to produce particles at the electroweak scale. Using the LHC as a photon collider, the ATLAS collaboration announced a set of landmark results at the 40th International Conference on High Energy Physics last week, among which is the first observation of the photo-production of W-boson pairs.

As it proceeds via trilinear and quartic gauge-boson vertices involving two W bosons and either one or two photons, the production of a pair of W bosons from two photons ($\gamma\gamma \to$ WW) tests a longstanding prediction

CERNCOURIER

Keep in touch: follow us on Twitter

- New results report the production of particles at the electroweak mass scale from photons
- With $\gamma\gamma \to WW$ serving as a fundamental test of electroweak theory
- Utilising the LHC run-2 pp dataset

Part I: The Theory

The Standard Model

- The Standard Model describes the fundamental constituents of matter and their interactions
  - strong and electroweak (EW) interaction
- Rich variety of interactions derived from a rather simple set of symmetries

- Electroweak symmetry is broken

$\rightarrow$ Mediators of the electroweak force have mass

- Self-interactions of electroweak gauge bosons
  - Quantum corrections at EW mass scale (probed in W/Z precision measurements)
  - Large effects at highest energies

- At the LHC we can test the electroweak theory at highest energies

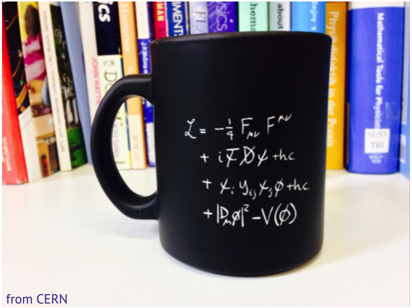

from CERN

$$\mathrm{SU}(3)_C \times \mathrm{SU}(2)_L \times \mathrm{U}(1)_Y$$

$\mathrm{SU}(3)_C$	$\mathrm{SU}(2)_L$	$\mathrm{U}(1)_Y$
colour red, green, blue	weak isospin $I_3 = 0, \pm\frac{1}{2}$	weak hypercharge Y
8 gluons	W^1, W^2, W^3	B

$\rightarrow W^+, W^-, Z, \gamma$

Electroweak Theory

- Gauge couplings arise from the SU(2) potential term $\mathcal{L} = -\frac{1}{4} W^a_{\mu\nu} W^{\mu\nu}_a$, with the field strength tensor $W^a_{\mu\nu} = \partial_\mu W^a_\nu - \partial_\nu W^a_\mu - g f_{abc} W^b_\mu W^c_\nu$
- It generates cubic and quartic couplings

$$
\begin{aligned}
\mathcal{L}_3 &= i e_{V=\gamma,Z} \left[W^+_{\mu\nu} W^{-\mu} V^\nu - W^-_{\mu\nu} W^{+\mu} V^\nu + W^+_\mu W^-_\nu V^{\mu\nu} \right] \\
\mathcal{L}_4 &= e_W^2 \quad \left[W^-_\mu W^{+\mu} W^-_\nu W^{+\nu} - W^-_\mu W^{-\mu} W^+_\nu W^{+\nu} \right] \\
&+ e^2_{V=\gamma,Z} \left[W^-_\mu W^{+\mu} V_\nu V^\nu - W^-_\mu V^\mu W^+_\nu Z^\nu \right] \\
&+ e_\gamma e_Z \left[2 W^-_\mu W^{+\mu} Z_\nu A^\nu - W^-_\mu Z^\mu W^+_\nu A^\nu - W^-_\mu A^\mu W^+_\nu Z^\nu \right]
\end{aligned}
$$

- With precise predictions of the coupling strength:

$e_\gamma = g \sin\theta_W$, $e_W = \dfrac{e_\gamma}{2\sqrt{2}\sin\theta_W}$ and $e_Z = e_\gamma \cot\theta_W$

- They *always* involve a pair of W bosons, there are no neutral vertices
- Heavy gauge bosons also couple to the Higgs boson

$$\mathcal{L}_{\text{Higgs}} = \frac{m_W^2}{v^2} W^+_\mu W^{-\mu} h^2 + \frac{m_Z^2}{v^2} Z_\mu Z^\mu h^2$$

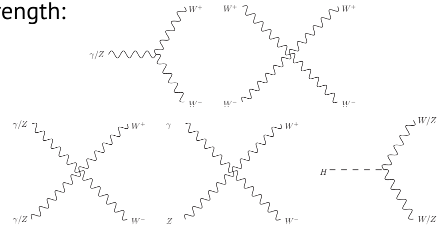

Gauge Cancellations

- Gauge-boson self interactions play a crucial role for the renormalisability of the electroweak theory
- Large cancellations of divergences arising in individual diagrams are exact if couplings take the values of the SM

$\rightarrow$ Diboson measurements are a sensitive probe of the inner structure of the electroweak symmetry

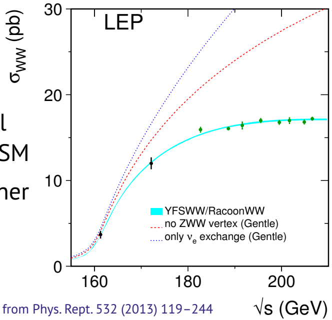

from Phys. Rept. 532 (2013) 119–244

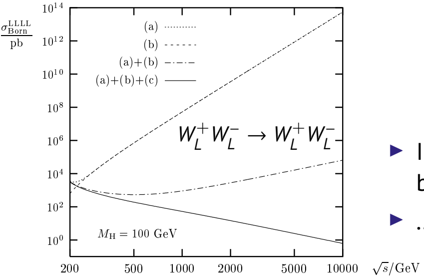

from Nucl. Phys. B525 (1998) 27-50

- In processes involving quartic couplings, the Higgs boson is governing the high energy behaviour
- ... if only W and Z bosons are involved

Vector-boson Scattering

- Measurements of processes with quartic electroweak couplings have already been established
- Electroweak diboson production, $V\,Vjj$

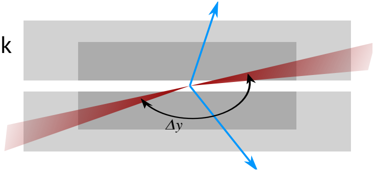

- The same final state can be produced in:
  - purely electroweak interactions involving only cubic and quartic self interactions
  - purely electroweak interactions without self interactions
  - processes involving both strong and electroweak interactions
- Electroweak production has characteristic signature of vector-boson scattering
- They are amongst the rarest reactions measured at the LHC so far ($\sigma = \mathcal{O}(1\text{ fb})$)

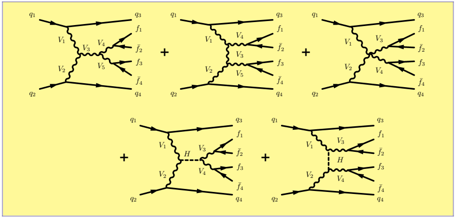

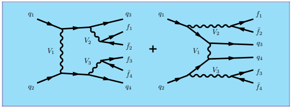

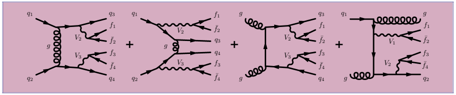

Experimental Status

- Electroweak $VVjj$ production has been experimentally confirmed for $ZZjj$, $WZjj$, $W^{\pm}W^{\pm}jj$, $W\gamma jj$ (and there's strong evidence for $Z\gamma jj$)

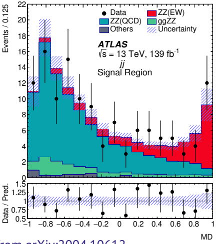

from arXiv:2004.10612

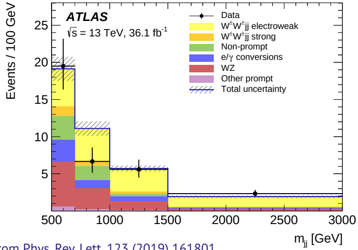

from Phys. Rev. Lett. 123 (2019) 161801

$$\sigma^{\text{fid}}_{W^{\pm}W^{\pm}jj\text{-EWK}} = 2.89 \pm 0.50\ (\text{stat}) \pm 0.29\ (\text{syst})\ \text{fb}$$
$$\sigma^{\text{fid}}_{W^{\pm}Zjj\text{-EWK}} = 0.57 \pm 0.14\ (\text{stat}) \pm 0.07\ (\text{syst})\ \text{fb}$$
$$\sigma^{\text{fid}}_{ZZjj\text{-EWK}} = 0.82 \pm 0.21\ (\text{syst})\ \text{fb}\ (4\ell \text{ and } 2\ell 2\nu)$$

- Strong production cross sections are typically orders of magnitude larger than those for electroweak production
- $W^{\pm}W^{\pm}jj$ production is *unique* in that strong production and electroweak diagrams without self interactions are suppressed
- ... and even more so is $\gamma\gamma \to WW$

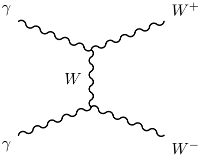

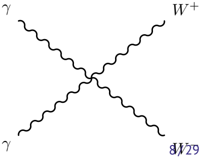

Photon-induced Processes

- Boosted charged particles are an intense source of “quasi-real” photons (Equivalent Photon Approximation)
- Longitudinal components of $\vec{E}$ and $\vec{B}$ vanish for $v \to c$

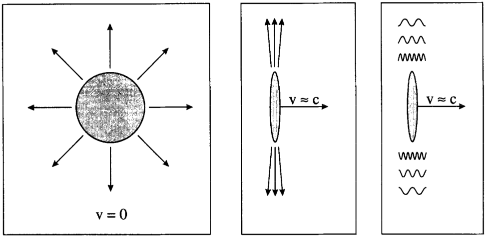

from Prog. Part. Nucl. Phys. **39** (1997), 503

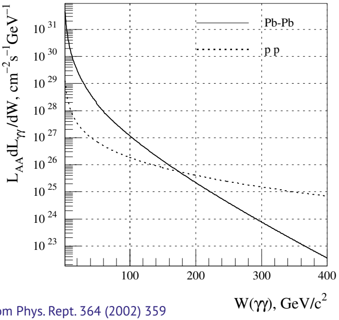

from Phys. Rept. 364 (2002) 359
(with outdated LHC design parameters)

Lead–lead vs proton–proton:

- Many studies of photon-induced processes use heavy-ion collisions
- Photon luminosity scales with $\sim Z^4$
- Maximum photon energy $\sim \gamma/R$ (uncertainty principle)

→ Use *pp* data to produce particles at electroweak mass scales or higher

Types of Photon-Photon Reactions

elastic

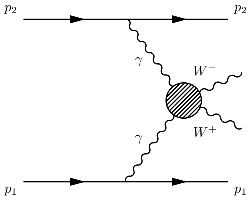

16%

semi-dissociative

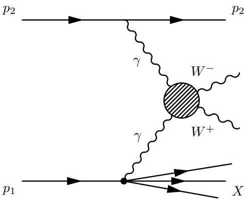

81%

double-dissociative

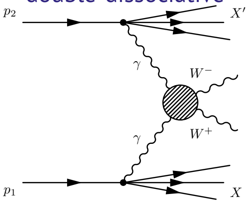

3%

- In practise, the photon radiation can lead to a breakup of the photon
- Factorisation into elastic form factors and DIS structure functions
  (see e.g. LUXqed approach, JHEP 12 (2017), 046)
- For elastic production, only, the protons stay intact and no particles except for W boson decay products are produced

→ Measurement maximizes acceptance of elastic production, requiring no further *reconstructed* particles

- Rescattering of proton can cause loss of signal

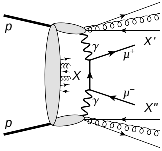

Part II: The Measurement

Analysis in a Nutshell

Experimental Signature:

- exactly one electron and muon with opposite electric charge
- $p_{\mathrm{T}}(ll) > 30$ GeV, $m_{\ell\ell} > 20$ GeV
- no charged particles associated with the primary interaction vertex

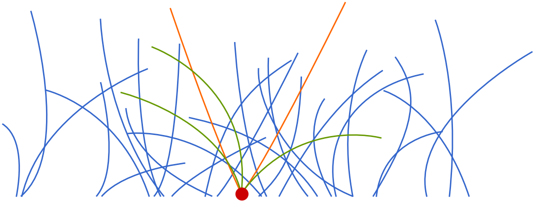

Experimental Challenges:

- In a typical ATLAS event we have a primary interaction vertex, and particles from the hard interaction, the proton fragmentation and additional *pp* interactions
- The analysis requires detailed understanding of:
  - vertex reconstruction ●
  - modelling of signal ●
  - the pileup density and multiplicity ●
  - underlying event of background processes ●

Track Reconstruction

- Accurately reconstructing as many charged-particle tracks as possible is key!
- Innermost tracking layer at $r = 33.5$ mm (pixel size: $50 \times 250\ \mu\text{m}^2$, intrinsic spacial resolution: $10 \times 75\ \mu\text{m}^2$)
- Tracks for analysis are selected with $d_0 < 1$ mm and $z_0 < 1$ mm

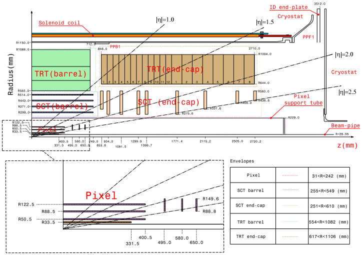

from JINST 12 (2017) P12009

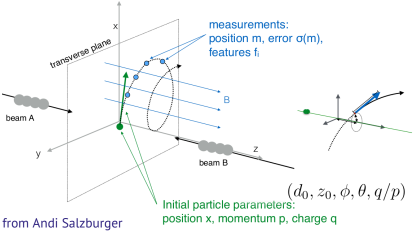

from Andi Salzburger

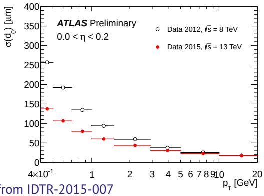

from IDTR-2015-007

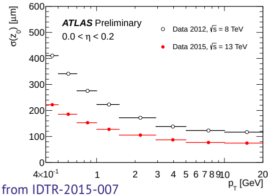

from IDTR-2015-007

Track Selection

- Tracks are the largest consumer of CPU in ATLAS reconstruction, and of disk space
- Only tracks with $p_T > 500$ MeV are available for analysis

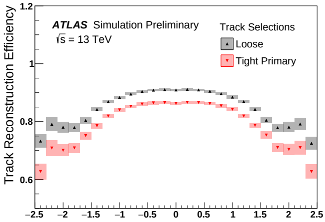

from ATL-PHYS-PUB-2015-051

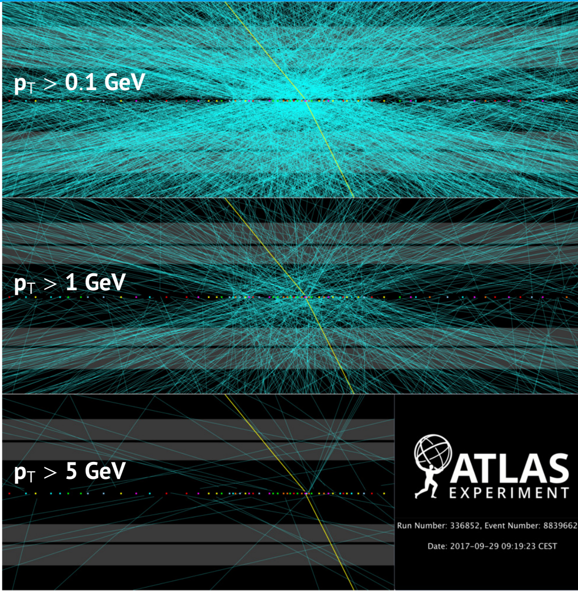

Vertex Reconstruction

- Usually, the interaction vertices are reconstructed from charged-particle tracks in the inner detector
- The vertex with the largest $\sum p_T^2$ is chosen as the primary vertex

→ Not optimal for photon-induced processes

- Instead, leptons are used to reconstruct the interaction vertex:

$$z_{\text{vtx}}^{\ell\ell} = \frac{z_{\ell_1} \sin^2\theta_{\ell_1} + z_{\ell_2} \sin^2\theta_{\ell_2}}{\sin^2\theta_{\ell_1} + \sin^2\theta_{\ell_2}}$$

  where $\sin^{-1}\theta_\ell$ parametrises the uncertainty of the measured z_ℓ position
- This vertex is *unbiased* by close-by pileup tracks
- and *more efficient* than the usual $\sum p_T^2$ criterion

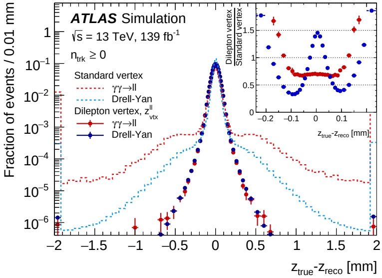

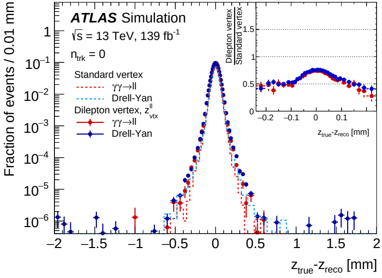

Pileup Challenge

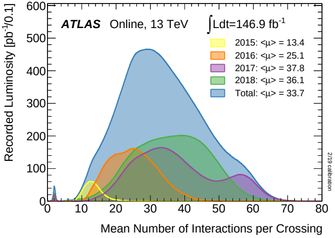

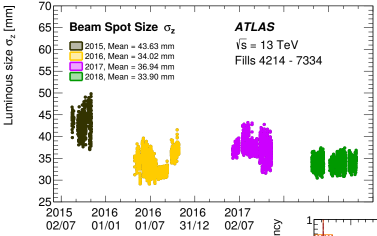

- Between 2015 and 2018 ATLAS recorded 139 fb^{-1} of *pp* collision data
  - With an average of 33.7 collisions per bunch crossing
  - With varying beam conditions
- A pileup vertex in the vicinity of the $\gamma\gamma \to WW$ vertex causes the event to be dropped
- Measurement relies on the correct description of the multiplicity and density of pileup tracks

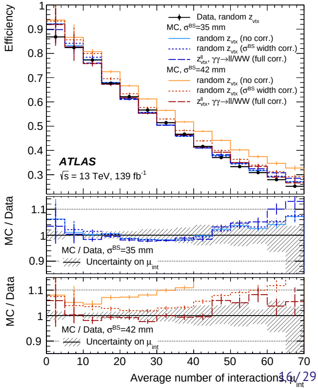

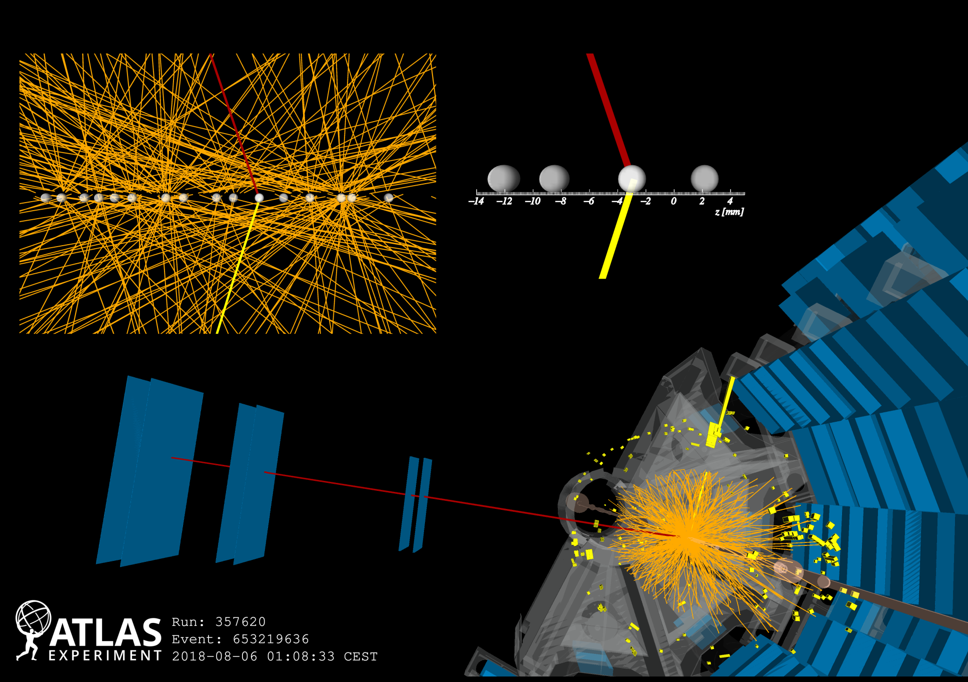
−14 −12 −10 −8 −6 −4 −2 0 2 4
z [mm]
ATLAS
EXPERIMENT
Run: 357620
Event: 653219636
2018-08-06 01:08:33 CEST

Pileup Modelling

- The probability of finding a pileup track within 1 mm of the vertex is 47.4%

→ Large source of efficiency loss

- Measured from several z-positions in Drell-Yan events, weighted with beam-spot distribution

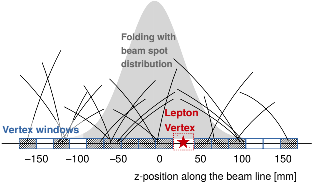

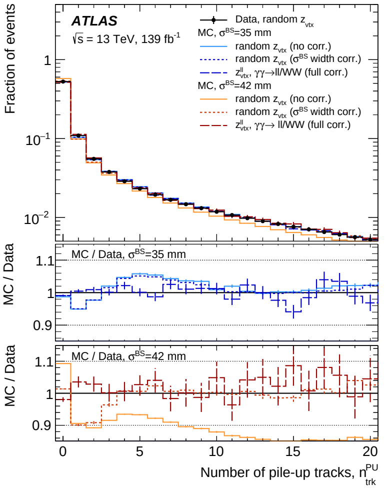

- Small differences between data and simulation are used as a correction, after correcting the beam-spot size

Background Modelling

- An accurate estimation of the backgrounds relies on the modelling of the underlying event
- Dominated by low-p_T, non-perturbative physics

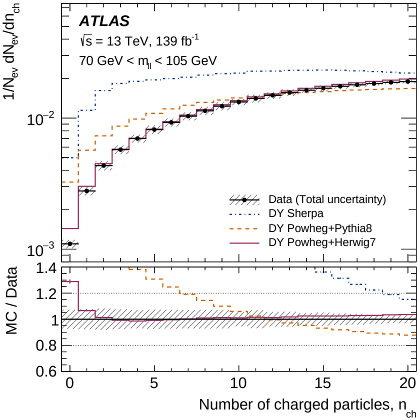

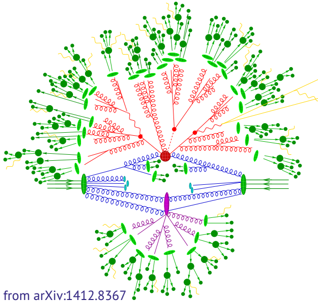

from arXiv:1412.8367

- The number of charged particles is measured in Drell-Yan events
- Double differentially in n_{ch} and $p_T(ll)$
- Separately for all parton shower models used in the analysis

Modelling of $qq \to WW$ Production

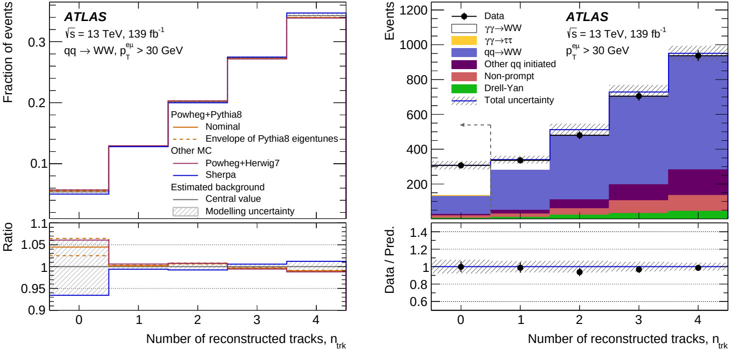

- Underlying event corrections derived in Drell-Yan events are used to correct $qq \to VV$ events, as a function of n_{ch} and $p_{\mathrm{T}}(VV)$
- Pythia8 eigentune vars., Herwig7 and Sherpa parton-shower models agree within 1% ... except for $n_{\mathrm{track}} = 0$

Differences are the largest source of uncertainty in the measurement

(with the $qq \to VV$ yield estimated from the average and envelope of the highest and lowest number)

Signal Modelling

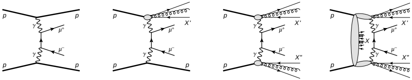

- No complete simulation of $\gamma\gamma \to WW$ available (or have only recently become available)
- In particular, no rescattering of the proton

$\rightarrow$ Measure missing components in $\gamma\gamma \to \ell\ell$

- Using elastic contributions for signal predictions, only

$$\beta_{\gamma\gamma\to\ell\ell} = \frac{N_{\text{data}} - N_{\text{bkg}}}{N^{\text{elastic}}_{\gamma\gamma\to\ell\ell}} = 3.59 \pm 0.15 \text{ (stat.+syst.)}$$

- Applicability to $\gamma\gamma \to WW$ ensured with $m_{\ell\ell} > 160$ GeV $\sim 2 \cdot m_W$ (and a generous uncertainty)

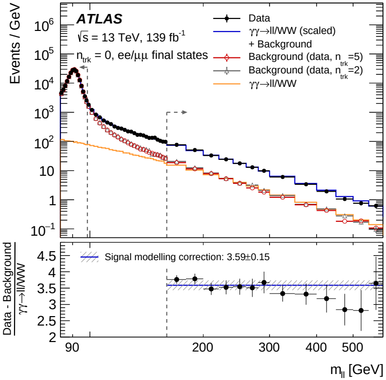

This approach assumes that the fraction of elastic and dissociative components are the same in $\gamma\gamma \to \ell\ell$ and $\gamma\gamma \to WW$ events, for a given $m_{\gamma\gamma}$

The Observation

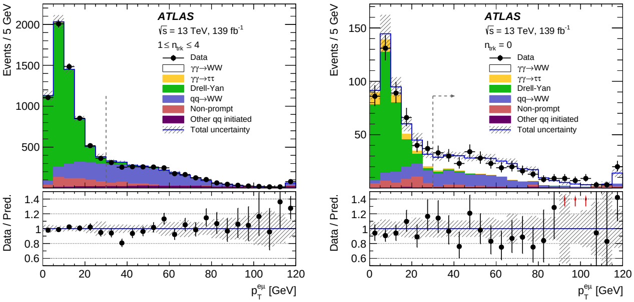

$$\beta_{WW} = 1.21^{+0.19}_{-0.23}$$
$$\beta_{\text{Drell-Yan}} = 1.16^{+0.10}_{-0.12}$$
$$\beta_{\gamma\gamma\to\ell\ell} = 3.59 \pm 0.15$$
$$\mu_{\gamma\gamma\to WW} = 1.33$$
$$\pm\, 0.14\ (\text{stat.})\ {}^{+0.22}_{-0.17}\ (\text{syst.})$$

- Signal extracted in a profile likelihood fit, using
  - four bins with $p_{\mathrm{T}}(ll) < 30$ GeV or $p_{\mathrm{T}}(ll) > 30$ GeV, and $1 \leq n_{\text{track}} \leq 4$ or $n_{\text{track}} = 0$
  - one bin for the signal modelling correction, $n_{\text{track}} = 0$ and $m_{\ell\ell} > 160$ GeV
  - four free parameters, the normalisations of $\gamma\gamma \to WW$, $\gamma\gamma \to \ell\ell$, Drell-Yan and $qq \to WW$
- 307 candidate events are selected in data where 127 are expected from background

The background-only hypothesis is rejected with 8.4σ (6.7σ expected)

Fiducial Cross Section

- The fiducial cross section ($n_{\text{ch}} = 0$ + kinematic requirements) is measured to be

$$\sigma_{\text{meas.}} = 3.13 \pm 0.31\ (\text{stat.}) \pm 0.28\ (\text{syst.})\ \text{fb}$$

- Largest sources of uncertainty
  - Stat. uncertainties in the backgrounds
  - Background modelling
  - Signal modelling (dissociative contributions)
- Compared to our "expectation"

$$\sigma_{\text{elastic}} \cdot \beta_{\gamma\gamma\to\ell\ell} = 2.34 \pm 0.27\ \text{fb}$$

- A standalone prediction from Madgraph with MMHT2015qed PDF

$$\sigma_{\text{theo.}} = 4.3 \pm 1.0\ (\text{scale}) \pm 0.12\ (\text{PDF})\ \text{fb}$$

- This value needs to be corrected for rescattering effects ranging between 0.65 and 0.82

Source of uncertainty	Impact [%]
Experimental	
Track reconstruction	1.1
Electron energy scale and resolution, and efficiency	0.4
Muon momentum scale and resolution, and efficiency	0.5
Misidentified leptons	1.5
Background, statistical	6.7
Modelling	
Pile-up modelling	1.1
Underlying-event modelling	1.4
Signal modelling	2.1
WW modelling	4.0
Other backgrounds	1.7
Luminosity	1.7
Total	8.9

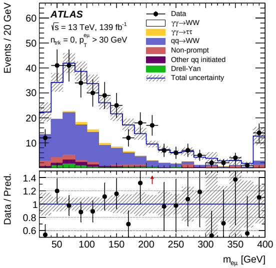

Part III: The Future

ATLAS Forward Proton Detectors

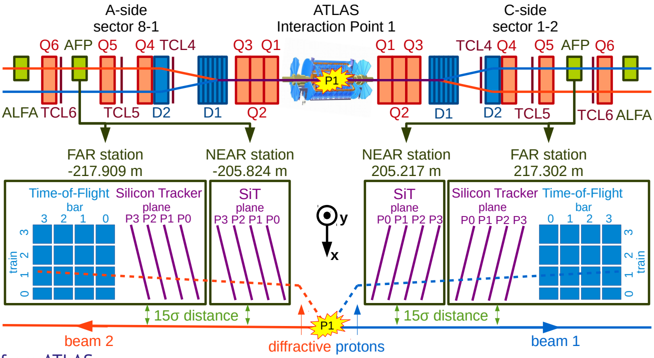

from ATLAS

- The AFP spectrometer is among newest additions to ATLAS (installed between 2016 and 2017)
- Direct detection of scattered protons that leave the interaction intact
- Reconstruction of relative proton energy loss from the deflection in LHC magnetic field

$$\xi = 1 - E_{\text{scattered}}/E_{\text{beam}}$$

with an acceptance of $0.02 < \xi < 0.1$

Observation of Proton-tagged Dilepton Production

- Measurement of $pp \to p(\gamma\gamma \to \ell\ell)p^{(*)}$
- Using part of 2017 data

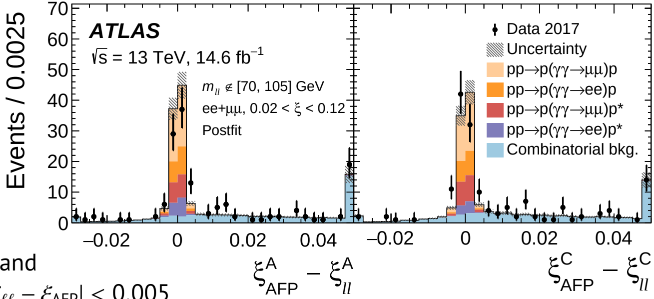

- Observation of 57 $ee + p$ and 123 $\mu\mu + p$ events with $|\xi_{\ell\ell} - \xi_{\text{AFP}}| < 0.005$
- Pioneering work on performance measurements and analysis techniques
- Systematic uncertainties in alignment, resolution and knowledge of beam optics of 9%

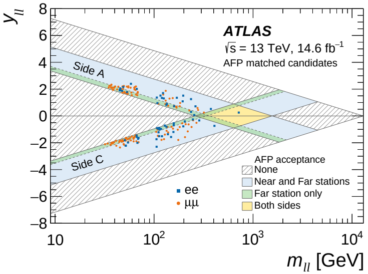

The measurement introduces forward proton tagging in cross-section measurements of photon-fusion processes

Standard Model Effective Field Theory

- Make use of Standard Model measurements to constrain new physics
- Quantify agreement of couplings with SU(2)×U(1) prediction
- Expand Standard Model Lagrangian with higher dimension (of energy) operators Q_i
  (supressed by powers of inverse energy scale $1/\Lambda$)

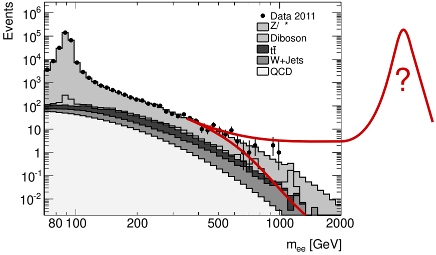

$$\mathcal{L}_{\text{SM EFT}} = \mathcal{L}_{\text{SM}} + \sum_i \frac{c_i^{\text{dim-6}}}{\Lambda^2} Q_i^{\text{dim-6}} + \sum_i \frac{c_i^{\text{dim-8}}}{\Lambda^4} Q_i^{\text{dim-8}}$$

(excluding lepton/baryon number violating operators)

- Only at dim-8 (or higher) there are operators which affect quartic but not cubic gauge couplings

Vertex \ Operator	O_{S0} O_{S1} O_{S2}	O_{M0} O_{M1} O_{M7}	O_{M2} O_{M3} O_{M4} O_{M5}	O_{T0} O_{T1} O_{T2}	O_{T5} O_{T6} O_{T7}	O_{T8} O_{T9}
$WWWW$	✓	✓		✓		
$WWZZ$	✓	✓	✓	✓	✓	
$WWZ\gamma$		✓	✓	✓	✓	
$WW\gamma\gamma$		✓	✓	✓	✓	
$ZZZZ$	✓	✓	✓	✓	✓	✓
$ZZZ\gamma$		✓	✓	✓	✓	✓
$ZZ\gamma\gamma$		✓	✓	✓	✓	✓
$Z\gamma\gamma\gamma$				✓	✓	✓
$\gamma\gamma\gamma\gamma$				✓	✓	✓

EFT parametrisation of O. Eboli, M. Gonzalez-Garcia (arxiv:1604.03555)

Prospects for $\gamma\gamma \rightarrow WW$

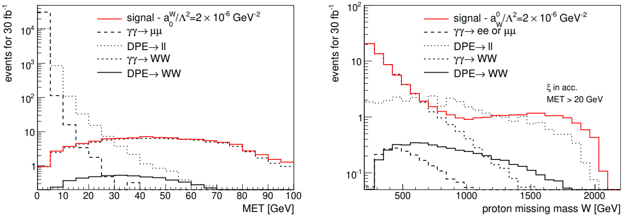

from Phys. Rev. D 81, 074003 (2010) from Phys. Rev. D 81, 074003 (2010)

- Forward proton tagging allows reconstruction of the WW system in $\gamma\gamma \rightarrow WW$ events

$$W = \sqrt{s\xi_1\xi_2} = m_{WW}$$

- With acceptance of 300 GeV $< W <$ 1.5 TeV of double-tagged events

- Possibility to measure differential cross section as a function of $m_{\gamma\gamma}$

$\rightarrow$ Increased sensitivity for EFT interpretations in LHC run-3

Summary

- There is a vibrant and emerging physics program using the LHC as a photon collider
- Progress in experimental techniques allow use of high pileup *pp* data

- The production of two W bosons from two photons has been observed
- As it proceeds through quartic gauge couplings, it confirms a longstanding Standard Model prediction

- Have a look at our paper arXiv:2010.04019

Backup

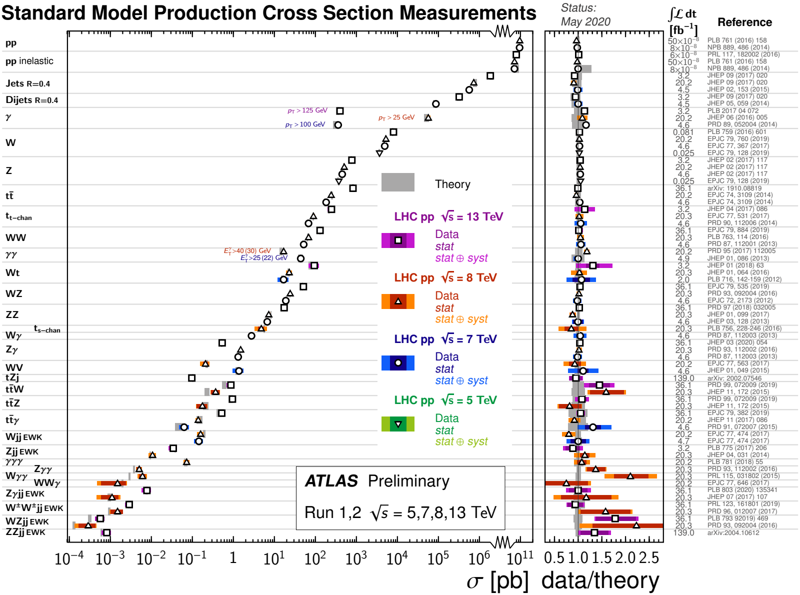
Standard Model Production Cross Section Measurements
Status: May 2020
∫ℒ dt [fb⁻¹]
Reference
pp
pp inelastic
Jets R=0.4
Dijets R=0.4
γ
W
Z
tt̄
t_t−chan
WW
γγ
Wt
WZ
ZZ
t_s−chan
Wγ
Zγ
WV
tZj
tt̄W
tt̄Z
tt̄γ
Wjj EWK
Zjj EWK
γγγ
Zγγ
Wγγ
WWγ
Zγjj EWK
W±W±jj EWK
WZjj EWK
ZZjj EWK
p_T > 125 GeV
p_T > 100 GeV
p_T > 25 GeV
E_T^γ>40 (30) GeV
E_T^γ>25 (22) GeV
Theory
LHC pp √s = 13 TeV
Data
stat
stat ⊕ syst
LHC pp √s = 8 TeV
Data
stat
stat ⊕ syst
LHC pp √s = 7 TeV
Data
stat
stat ⊕ syst
LHC pp √s = 5 TeV
Data
stat
stat ⊕ syst
ATLAS Preliminary
Run 1,2 √s = 5,7,8,13 TeV
10⁻⁴ 10⁻³ 10⁻² 10⁻¹ 1 10¹ 10² 10³ 10⁴ 10⁵ 10⁶ 10¹¹
σ [pb]
0.5 1.0 1.5 2.0 2.5
data/theory
50×10⁻⁸ PLB 761 (2016) 158
8×10⁻⁸ NPB 889, 486 (2014)
6×10⁻⁸ PRL 117, 182002 (2016)
50×10⁻⁸ PLB 761 (2016) 158
8×10⁻⁸ NPB 889, 486 (2014)
3.2 JHEP 09 (2017) 020
20.2 JHEP 09 (2017) 020
4.5 JHEP 02, 153 (2015)
3.2 JHEP 09 (2017) 020
4.5 JHEP 05, 059 (2014)
3.2 PLB 2017 04 072
20.2 JHEP 06 (2016) 005
4.6 PRD 89, 052004 (2014)
0.081 PLB 759 (2016) 601
20.2 EPJC 79, 760 (2019)
4.6 EPJC 77, 367 (2017)
0.025 EPJC 79, 128 (2019)
3.2 JHEP 02 (2017) 117
20.2 JHEP 02 (2017) 117
4.6 JHEP 02 (2017) 117
0.025 EPJC 79, 128 (2019)
36.1 arXiv: 1910.08819
20.2 EPJC 74, 3109 (2014)
4.6 EPJC 74, 3109 (2014)
3.2 JHEP 04 (2017) 086
20.3 EPJC 77, 531 (2017)
4.6 PRD 90, 112006 (2014)
36.1 EPJC 79, 884 (2019)
20.3 PLB 763, 114 (2016)
4.6 PRD 87, 112001 (2013)
20.2 PRD 95 (2017) 112005
4.9 JHEP 01, 086 (2013)
3.2 JHEP 01 (2018) 63
20.3 JHEP 01, 064 (2016)
2.0 PLB 716, 142-159 (2012)
36.1 EPJC 79, 535 (2019)
20.3 PRD 93, 092004 (2016)
4.6 EPJC 72, 2173 (2012)
36.1 PRD 97 (2018) 032005
20.3 JHEP 01, 099 (2017)
4.6 JHEP 03, 128 (2013)
20.3 PLB 756, 228-246 (2016)
4.6 PRD 87, 112003 (2013)
36.1 JHEP 03 (2020) 054
20.3 PRD 93, 112002 (2016)
4.6 PRD 87, 112003 (2013)
20.2 EPJC 77, 563 (2017)
4.6 JHEP 01, 049 (2015)
139.0 arXiv: 2002.07546
36.1 PRD 99, 072009 (2019)
20.3 JHEP 11, 172 (2015)
36.1 PRD 99, 072009 (2019)
20.3 JHEP 11, 172 (2015)
36.1 EPJC 79, 382 (2019)
20.2 JHEP 11 (2017) 086
4.6 PRD 91, 072007 (2015)
20.2 EPJC 77, 474 (2017)
4.7 EPJC 77, 474 (2017)
3.2 PLB 775 (2017) 206
20.3 JHEP 04, 031 (2014)
20.2 PLB 781 (2018) 55
20.3 PRD 93, 112002 (2016)
20.3 PRL 115, 031802 (2015)
20.2 EPJC 77, 646 (2017)
36.1 PLB 803 (2020) 135341
20.3 JHEP 07 (2017) 107
36.1 PRL 123, 161801 (2019)
20.3 PRD 96, 012007 (2017)
36.1 PLB 793 92019) 469
20.3 PRD 93, 092004 (2016)
139.0 arXiv:2004.10612

	Signal region		Control regions	
n_{trk}	$n_{\mathrm{trk}} = 0$		$1 \leq n_{\mathrm{trk}} \leq 4$	
$p_{\mathrm{T}}^{e\mu}$	> 30 GeV	< 30 GeV	> 30 GeV	< 30 GeV
$\gamma\gamma \to WW$	174 ± 20	45 ± 6	95 ± 19	24 ± 5
$\gamma\gamma \to \ell\ell$	5.5 ± 0.3	39.6 ± 1.9	5.6 ± 1.2	32 ± 7
Drell–Yan	4.5 ± 0.9	280 ± 40	106 ± 19	4700 ± 400
$qq \to WW$ (incl. gg and VBS)	101 ± 17	55 ± 10	1700 ± 270	970 ± 150
Non-prompt	14 ± 14	36 ± 35	220 ± 220	500 ± 400
Other backgrounds	7.1 ± 1.7	1.9 ± 0.4	311 ± 76	81 ± 15
Total	305 ± 18	459 ± 19	2460 ± 60	6320 ± 130
Data	307	449	2458	6332

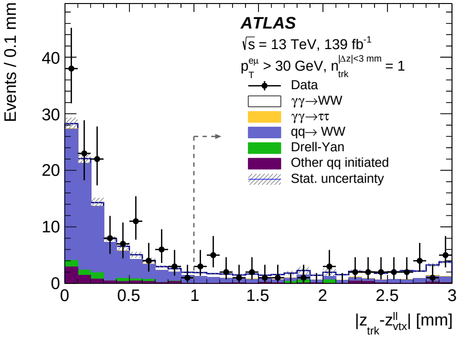
ATLAS
√s = 13 TeV, 139 fb^-1
p_T^eμ > 30 GeV, n_trk^|Δz|<3 mm = 1
Data
γγ→WW
γγ→ττ
qq→ WW
Drell-Yan
Other qq initiated
Stat. uncertainty
Events / 0.1 mm
|z_trk-z_vtx^ll| [mm]
0
10
20
30
40
0.5
1
1.5
2
2.5
3

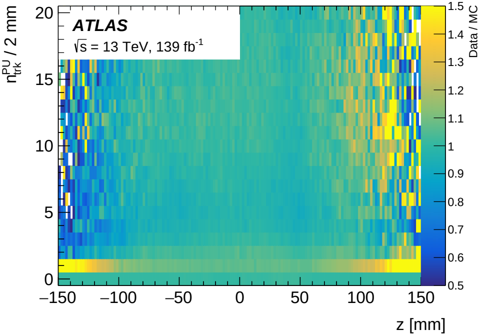
ATLAS
$\sqrt{s}$ = 13 TeV, 139 fb^{-1}
n^{PU}_{trk} / 2 mm
z [mm]
Data / MC
20
15
10
5
0
–150
–100
–50
0
50
100
150
1.5
1.4
1.3
1.2
1.1
1
0.9
0.8
0.7
0.6
0.5

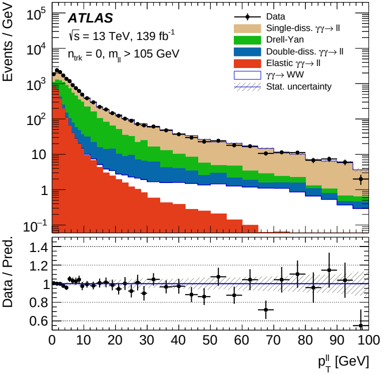
ATLAS
√s = 13 TeV, 139 fb-1
ntrk = 0, mll > 105 GeV
Data
Single-diss. γγ→ ll
Drell-Yan
Double-diss. γγ→ ll
Elastic γγ→ ll
γγ→ WW
Stat. uncertainty
Events / GeV
Data / Pred.
pTll [GeV]

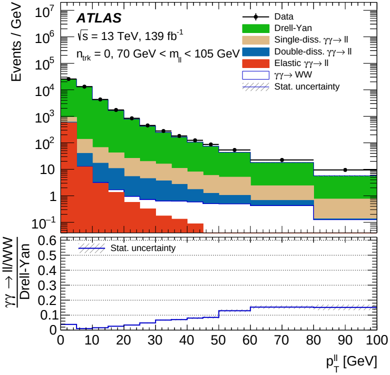
ATLAS
√s = 13 TeV, 139 fb-1
ntrk = 0, 70 GeV < mll < 105 GeV
Data
Drell-Yan
Single-diss. γγ→ ll
Double-diss. γγ→ ll
Elastic γγ→ ll
γγ→ WW
Stat. uncertainty
Events / GeV
γγ → ll/WW / Drell-Yan
pTll [GeV]